Schweizerische Eidgenossenschaft
Confédération suisse
Confederazione Svizzera
Confederaziun svizra

Eidgenössisches Departement für
Umwelt, Verkehr, Energie und Kommunikation UVEK

Bundesamt für Energie BFE

GEO-THERMOPOWER

GEO-TEP MATERIALS

Jahresbericht 2007

Autor und Koautoren	Laura Bocher and Anke Weidenkaff
beauftragte Institution	Empa
Adresse	Ueberlandstrasse 129
	CH-8600 Duebendorf. Switzerland
Telefon, E-mail, Internetadresse	+41 44 823 41 31, anke.weidenkaff@empa.ch
BFE Projekt-/Vertrag-Nummer	101356 / 151615
BFE-Projektleiter	Anke Weidenkaff
Dauer des Projekts (von – bis)	22.08.2005 – 15.03.2009
Datum	25.11.2007

ZUSAMMENFASSUNG

Orthorhombic perovskite-type $CaMn_{1-x}Nb_xO_{3-\delta}$ (x = 0.02, 0.05 and 0.08) were studied concerning their high temperature thermoelectric properties. Investigations on electrical resistivity, thermoelectric power and thermal conductivity of theses phases are reported concerning the synthesised compounds. The crystal structure and the cell parameters were determined by x-ray powder diffraction data (XRPD) for the different manganate phases. Either *"Chimie douce"* synthesis or classical solid state reaction methods were used to produce the oxides.

Differences in transport and thermal properties can be correlated to the different microstructures obtained by the two synthesis method. A small polaron hopping model can be applied for the high temperature resistivity behavior (T > 300 K). The electron doped manganate phases exhibit at high temperatures large absolute Seebeck coefficients (e.g. for x = 0.05: S_{1000K} = -180μV.K^{-1} and present low resistivity values (e.g. ρ_{1000K} = 16.8 m Ω.cm for x=0.05). A large power factor (PF) is achieved in the high temperature range (e.g. for x = 0.05, PF > 1.90 * 10^{-4} W.m^{-1}K^{-2} for 450 K < T < 1070 K). These PF values combined with low thermal conductivity values make these phases potential candidates as *n*-type thermoelectric elements at high temperatures.

Projektziele

Thermoelectric (TE) applications emerge nowadays as a potential technology allowing the conversion of heat into electric power. This energy conversion proceed presents the advantages to generate electricity without (i) using moving parts as gas turbine engines or (ii) any chemical conversion as Solid Oxide Fuel Cell (SOFC) devices [Stambouli 2002]. The TE modules do not require any additional maintenance. Oxide materials with promising TE activities are interesting due to (i) their chemical and thermal stability at high temperatures inducing long operating lifetime and (ii) the low cost of the raw materials, e.g. manganese, compared to the TE state-of-the-art materials e.g. Bi_2Te_3 or others tellurite-based compounds.

The efficient conversion of heat into electricity requires the development of materials exhibiting a high Figure of Merit, $Z = S^2/\rho\kappa$. Low level cationic or anionic substitutions allow to combine large Seebeck coefficients, *S,* with low electrical resistivity values, ρ, compared to the non-substituted parent compound [Maignan 1998]. A further challenge is to reduce the thermal conduction, κ, defining by the sum of the electronic component, κ_{el}, and the lattice contribution, $\kappa_{ph.}$ For oxide materials the phonon contribution remains the predominant component of the total thermal conductivity, therefore different strategies are investigated to lower the lattice heat conduction [Nolas].

The present report emphasizes the differences of morphological and microstructural features depending on the synthesis methods among the $CaMn_{1-x}Nb_xO_{3-\delta}$ series ($x < 0.10$). A good compromise is reached between the morphological fine-tuning and the three interrelated TE parameters (S, ρ and κ) to enhance the TE properties of the electron-doped manganate phases. Large thermopower coexists with semimetallic behavior at high temperatures making them prospective for the development of *n*-type thermoelements. Among the studied manganate-type phases, the compound presenting the best Figure of Merit in the precise temperature range was selected as *n*-type legs for the development of a Thermoelectric Oxide Module (TOM). The *p*-type leg was choosen among the cobaltate-type phases (cf project of Rosa Robert). Therefore the first generation TOM devices were built at Empa to test and optimize the maximum ouput power (cf project of Petr Tomes). As the geothermal processes allow to use small temperature gradients as renewable heat, the TOM devices based on oxide materials can convert directly the geothermal heat into electricity.

Durchgeführte Arbeiten und erreichte Ergebnisse

Polycrystalline perovskite-type phases $CaMn_{1-x}Nb_xO_3$ (with x = 0.02; 0.05 and 0.08) were synthesised by different *chimie douce* synthesis methods with emphasis on low synthesis temperature (873 K < T < 1073 K) [Weidenkaff 2004; Bocher 2007_A].

(i) **Stepwise calcinations (SC)** were applied to decompose in air the corresponding citrate precursor prepared by soft chemistry synthesis method leading to submicrometer particle size (see Figure 1 (a)) (cf Jahresbericht 2005 -2006).

(ii) **Ultrasonic Spray Combustion (USC)** method allows to decompose microdroplets of the precursor solution flowing in a high temperature furnace by a continuous process. Perovskite-type manganate phases are obtained as nano-crystallites with defined rectangle like shape (cf Jahresbericht 2006) [Bocher 2007_B].

(iii) A **Solid State Reaction (SSR)** process consists to synthesise polycrystalline powders by mixing carbonates or oxides and sintering at high temperatures T = 1673 K for 6h. The grain size is typically in the range of 3-10 μm (see Figure 1 (b)).

All synthesis methods lead to pure perovskite phases and allow to evaluate the microstructure impact on the transport properties. Different particle size and morphologies are achieved by these 3 synthesis methods. Electrical and thermal properties are further studied in correlation with the specific morphologies.

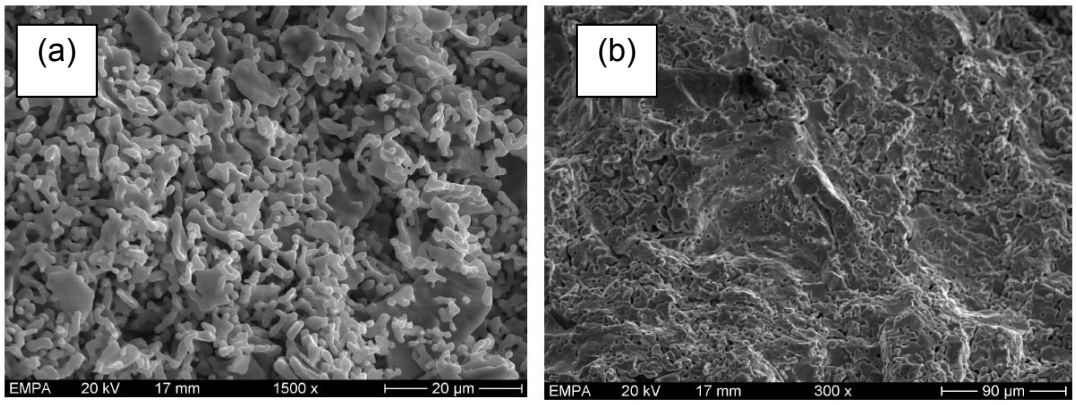

Figures 1: HRSEM images of $CaMn_{0.95}Nb_{0.05}O_3$ cross section sintered pellets synthesised by a) SC method and b) SSR method.

A) Structure and microstructure

The crystal structure and lattice parameters can be determined by Rietveld refinement method [Rietveld 1967] from the x-ray powder diffraction data (XRPD) (Figure 2). The structural parameters were refined for all the studied compositions, as reported in Table 1, confirming the orthorhombic crystal structure (S.G. *Pnma*). The Nb substitutions lead to an increase of the volume cell and lattice parameters due to an increase of the Mn^{3+} cation content in the $CaMnO_3$ matrix.

High temperatures XRPD measurements were performed (at ETHZ in collaboration with L. Castaldi and Prof. Ch. Baerlocher) for $CaMn_{0.98}Nb_{0.02}O_3$ compound as presented in the Figures 3. A transition occurs at T ~ 973 K where some reflexions clearly disappear from the transition temperature (see the arrows on the Figure 3 (a)). These first results suggest a phase transition from the orthorhombic to the rhombohedral or cubic structure. The refinements of the high temperatures data are still in progress and could be confirmed by a TEM study at high temperatures. The Figure 3 (b) shows a detail of the diffraction pattern for which the reflexions are shifted to the lower angles (see the red arrow on the Figure 3 (b)) due to thermal displacement at high temperatures.

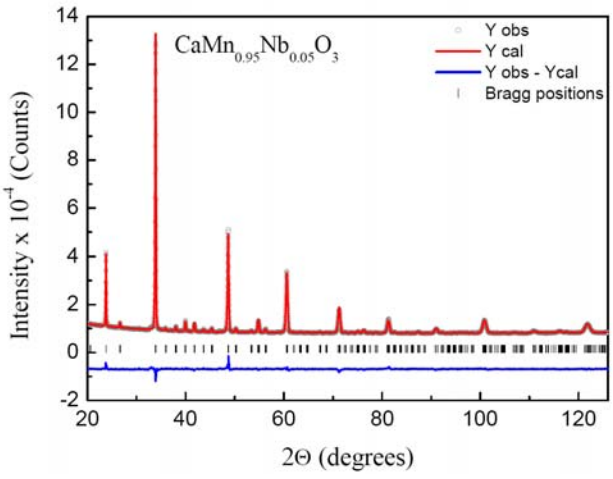

Figure 2: An example of a Rietveld refinement for $CaMn_{0.95}Nb_{0.05}O_3$ prepared by SC method. Orthorhombic crystal structure, P*nma* S.G. with unit cell parameters $a_p\sqrt{2}$ x $2a_p$ x $a_p\sqrt{2}$ (a_p corresponds to the perovskite cubic cell parameter with a_p ~ 3.7Å).

Composition	a (Å)	b (Å)	c (Å)	d^*	R_{wp}	R_p	χ^2
$CaMn_{0.98}Nb_{0.02}O_3$	5.2883 (2)	7.4647 (2)	5.2762 (2)	4.586	14.4	7.9	2.8
$CaMn_{0.95}Nb_{0.05}O_3$	5.3042 (3)	7.4802 (4)	5.2864 (2)	4.590	13.3	8.3	3.7
$CaMn_{0.92}Nb_{0.08}O_3$	5.3214 (3)	7.5010 (3)	5.2993 (2)	4.289	11.7	6.9	2.5

Table 1: Structural parameters for $CaMn_{1-x}Nb_xO_3$ (x = 0.02; 0.05; 0.08) refined from x-ray powder data. (d^* is the theoretical density ($g.cm^{-3}$).

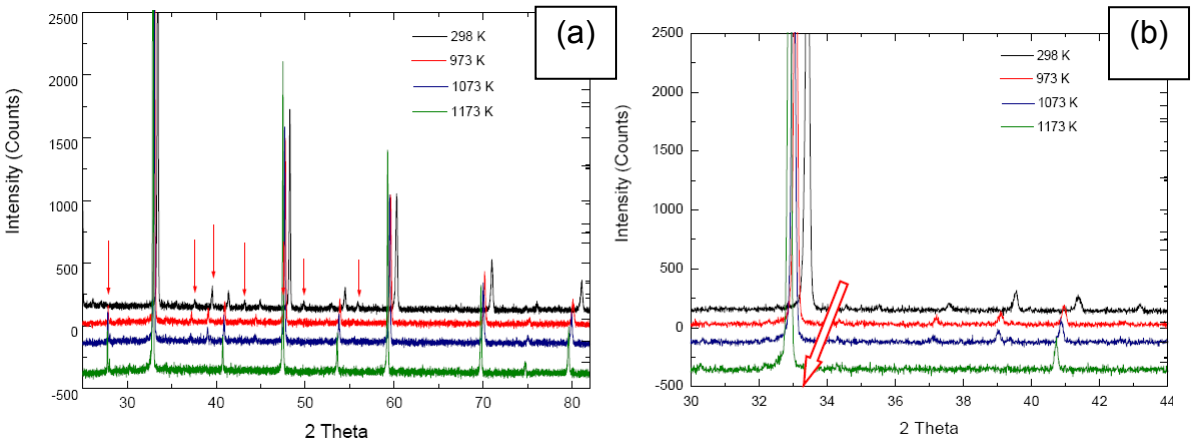

Figures 3 (a) and (b): High temperature XRPD measurements of $CaMn_{0.98}Nb_{0.02}O_3$ compound.

The Transmission Electron Microscopy (TEM) studies allow to confirm on a nanoscale level the structural information obtained from the Rietveld refinement. The High Resolution TEM images reflect the microstructure of the studied compound and the Electron Diffraction (ED) pattern allows to identify the crystallographic characteristic of the phases.

Different crystallites of the SC series were studied by TEM. As shown on the Figure 4, the HRTEM image presents highly crystalline perovskite structure without any apparent microstructural defect. The TEM studies of the same compound reveal a second type of microstructure on others crystallites (Figures 5 a) and b)). The Figure 5 (a) exhibits two distinct regions (A and B) for which the microstructure is composed by two twinned microdomains. The border between the two twinned domains is presented on the Figure 5 (b). The orthorhombic phases allows such twinning of the structure since the a and c lattice parameters present close values [Aguirre 2007]. Further studies on the presence of twinned domains related with the Nb substitution are planned to investigate the influence of the microdomains on the transport properties at high temperatures.

The USC particles sintered into pellets lead to nano-crystallites of 20-50 nm length presenting a defined rhomboid-like shape as shown in Figure 6 (a). The HRTEM image displays lattice granges corresponding to (010)o planes, in the orthorhombic framework, confirming the highly crystalline character of the manganate phases achieved from the USC particles. The experimental ED pattern (Figure 6 (b)) can be understood as the overlapping of twinned domains with two different *b* axis orientation in the orthorhombic structure corresponding to $[-101]_o$ + $[0-10]_o$ [ref].

To summarize the SC compounds as well as the USC nano-crystallites exhibit a well ordered crystalline microstructure associated to textural features with the presence of twinned domains.

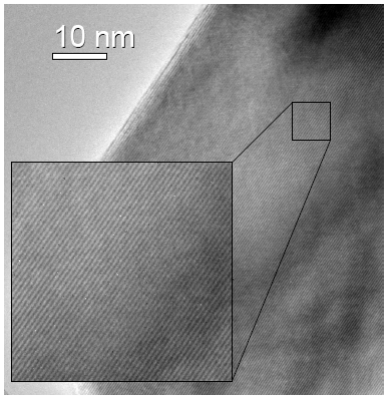

Figure 4: HRTEM of a long range crystalline structure of $CaMn_{0.95}Nb_{0.05}O_3$ synthesised by SC method.

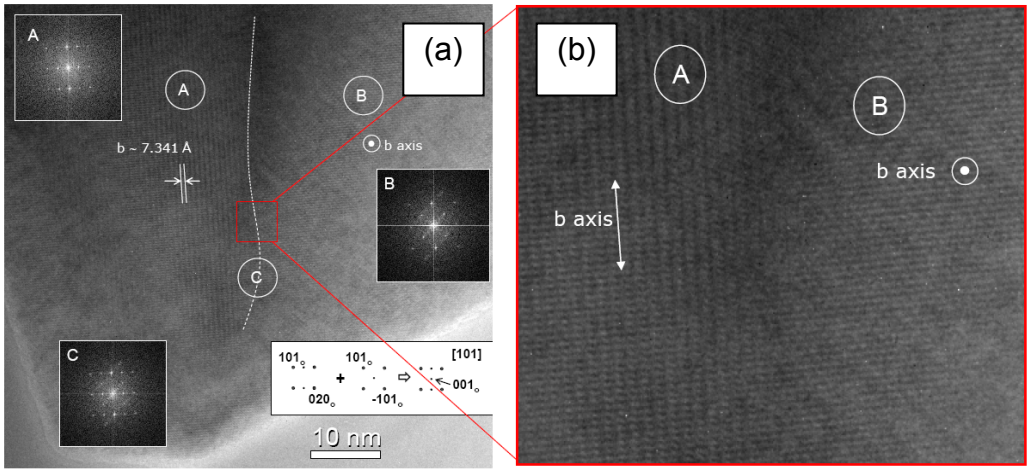

Figures 5: (a) HRTEM of twinned domains of $CaMn_{0.95}Nb_{0.05}O_3$ from the SC series. The inset figures present the Fast Fourier Transform (FFT) of the twinned domains A and B and the superposition of both in region C. (b) A zoom on the limit between the two domains A and B areas.

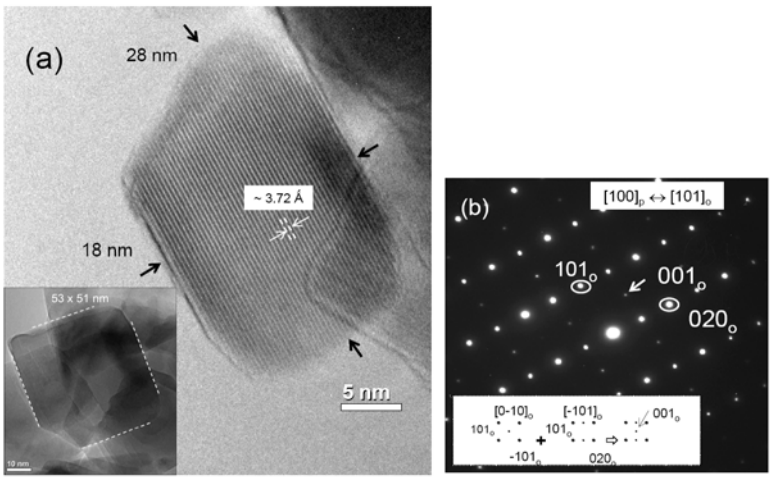

Figures 6: a) HRTEM image of nanocrystallite and b) ED of $CaMn_{0.98}Nb_{0.02}O_3$ sintered crystallites from USC particles. The zone axis can be related from the cubic (labelled "p") to the orthorhombic ("o") perovskite structure as $[100]_p \leftrightarrow [101]_o$. The ED pattern represents two twinned domains in different b axis directions.

B) Thermoelectric properties

Electrical resistivity

The introduction of Nb^{5+} cation on the *B*-site of $CaMnO_3$ induces the Mn^{3+} Jahn Teller cation formation in the Mn^{4+} matrix. The Figure 7 (a) displays the electrical resistivity versus temperature for all compounds. The transport properties change therefore gradually with temperature. At low temperature (T < 150 K) the resistivity increases with decreasing temperature indicating a semi-conducting like behaviour ($d\rho/dT < 0$). The resistivity evolution tends to a semi-metallic like behaviour at high temperature (200 K < T < 1100 K) leading to relatively low resistivity values for oxide materials, e.g. for x = 0.05: ρ_{400K} = 12.1 mΩ.cm. The introduction of pentavalent cation as Nb^{5+} generates Mn^{3+} species on the Mn sublattice reflected by a slight improvement of resistivity values decreasing from ρ_{500K} = 26 mΩ.cm with 2% Nb to ρ_{500K} = 11.3 mΩ.cm with 8% Nb.

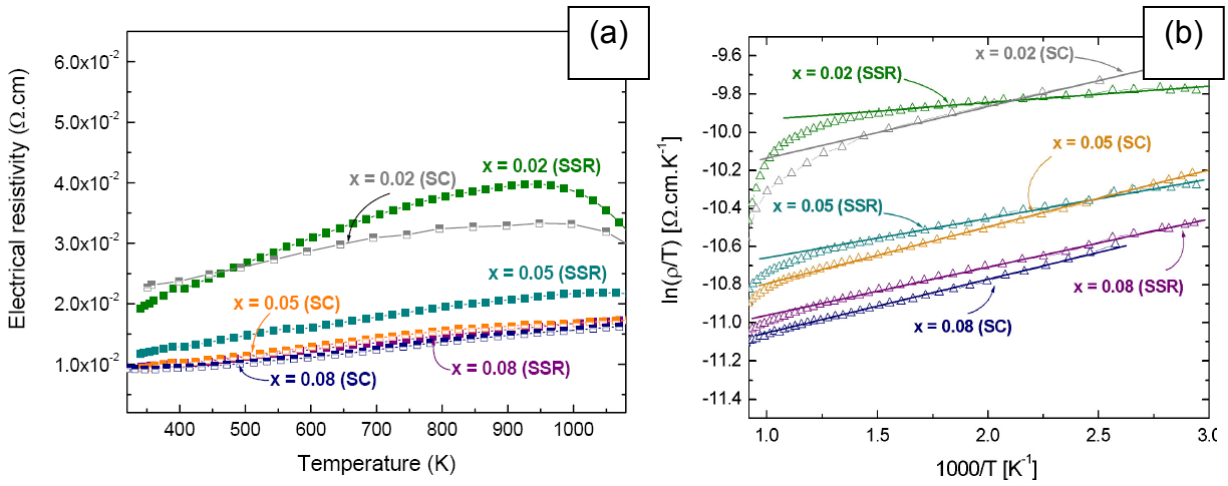

Figure 7: Evolution of resistivity as function of temperature in the high T range (T > 350 K) for $CaMn_{1-x}Nb_xO_3$ (for x = 0.02, 0.05 and 0.08) synthesised by SSR and SC methods.

The temperature resistivity dependence $\rho(T)$ are thermally activated and can be fitted for 320 K < T < 800 K with the relation: $\rho = AT^*(\exp Ea/k_B T)$ where *A* is a constant, *Ea* the activation of energy and k_B the Boltzmann constant. As previously reported [Maignan 1998, Hetjmanek 1999], the transport of carriers can be well described by the small polaron hopping conduction model, as shown in Figure 7 (b) where the fitting curves correspond to the experimental data. The fitting parameters are reported in Table 2 for all studied compounds. For the SSR series, the Nb content increase favors higher hopping energy values, e.g. Ea = 11.4 meV for 2\% Nb to Ea = 21.6 meV for 8\% Nb. This trend is also valid for the SC phases (see Table 2). To summarize the Nb substitution in the Mn sublattice favors lower resistivity values and the hopping energy increases indicating that higher concentration of Mn^{3+} Jahn Teller cations enhances the small polaron formation.

Different microstructures are obtained from SSR and SC synthesis which could affect the transport properties. Both series of compounds (SSR and SC) present the same resistivity temperature dependence, i.e. a metallic-like behavior. Nevertheless for equal Nb substitution the SC compounds exhibit lower ρ values compared to the SSR samples. The SC phases display also higher hopping energy values compared to the SSR compounds for equal Nb substitution, e.g for x = 0.05: Ea = 25.7 meV for SC phase and Ea =18.2 meV for SSR compound, emphasizing a enhancement of the carriers conduction for the SC phases due to an active small polaron hopping mechanism. Besides the SC series present lower relative densities than the SSR phases without affecting the electrical resistivity (Table 2). Submicrometer fine particles from SC synthesis methods lead to better connectivity between grains during the sintering process than for the SSR phases (cf HRSEM image: Figure 1 (a)). All these features indicate that the morphology and microstructure of the SC series appear more appropriate to transport charge carriers compared to the SSR compounds.

Niobium substitution	Mn valency	Synthesis method	Relative density	ρ (Ω.cm) at 800 K	A (Ω.cm)	Ea (meV)
0.02	3.98	SSR	80.20%	37.7	$4.10*10^{-5}$	11.4
		SC	68.7%	32.4	$3.07*10^{-5}$	22.84
0.05	3.94	SSR	82.90%	19.5	$1.52*10^{-5}$	17.5
		SC	67.7%	15.6	$1.50*10^{-5}$	25.7
0.08	3.91	SSR	85.61%	14.8	$1.35*10^{-5}$	21.6
		SC	77.3%	13.7	$1.81*10^{-5}$	24.8

Table 2: Transport properties fitting parameters depending on Nb substitutions and synthesis methods for the $CaMn_{1-x}Nb_xO_3$ series. (* Mn valency determined from expected composition $CaMn_{1-x}Nb_xO_3$ (x = 0.02; 0.05; 0.08))

Seebeck coefficient

All compounds present negative thermopower values for the whole temperature range (2 K < T < 1240 K) (see Figures 8 and 9) indicating electron as predominant charge carriers. Similar thermopower values and temperature dependence behaviour *S* (T) are reported for compounds with equal Nb substitutions either synthesised by SSR, USC or SC methods. This feature emphasizes that different polycrystalline natures and microstructures do not influence the intrinsic properties, i.e. charge carriers predominance. By increasing the Nb substitution on the Mn sublattice the absolute Seebeck values decrease from S_{900K} = -248μV.K^{-1} for x = 0.02 to S_{900K} = -150μV.K^{-1} for x = 0.08. The largest Seebeck values are reported for 2% Nb substitution where S_{1000K} = -251μV.K^{-1} for compounds prepared by both synthesis methods. At higher temperatures the absolute Seebeck values decrease suddenly from 1050 K which could be explained by the structural transition observed on the high temperatures XRDP data around 1000 K. The evaluations of the data are in progress.

Seebeck coefficients exhibit a linear temperature dependence in the paramagnetic region (200 K < T < 1000 K) for which absolute *S* values increase with temperature rising. The single band metal model can be applied for the $CaMn_{1-x}Nb_xO_3$ series in the high temperature range (200 K < T < 1000 K) [Hejtmanek 1999]. Theoretical Seebeck coefficients can be determined applying the single band metal model for a defined Nb substitution, e.g. S_{theo} = -130μV.K^{-1} for x = 0.05 and the $CaMn_{0.95}Nb_{0.05}O_3$ synthesised either by SSR or SC methods present a S_{exp} = -128μV.K^{-1} at 340 K.

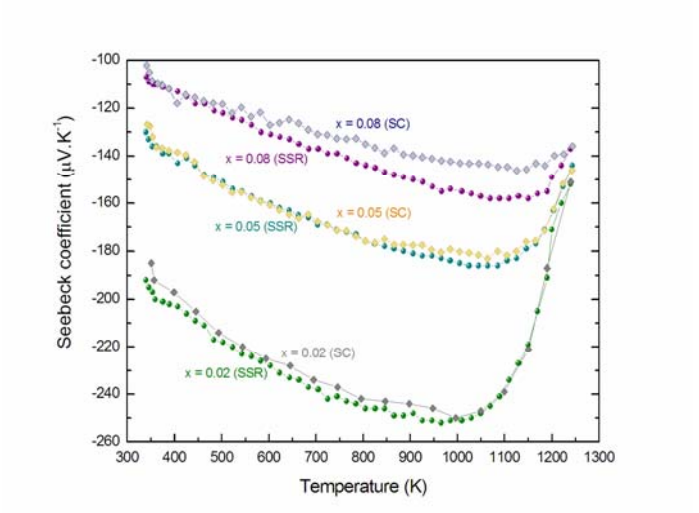

Figure 8: Temperature dependence of the Seebeck coefficient for $CaMn_{1-x}Nb_xO_3$ (for x = 0.02, 0.05 and 0.08) synthesised by SSR and SC methods.

In the case of the USC nano-crystallite, the compounds reveal a significant rise of the absolute Seebeck coefficients at T ~ 105 K (Figure 5 a)). This feature can be related to the pronounced suppression of the ferromagnetism fluctuations (Figure 5 b)).

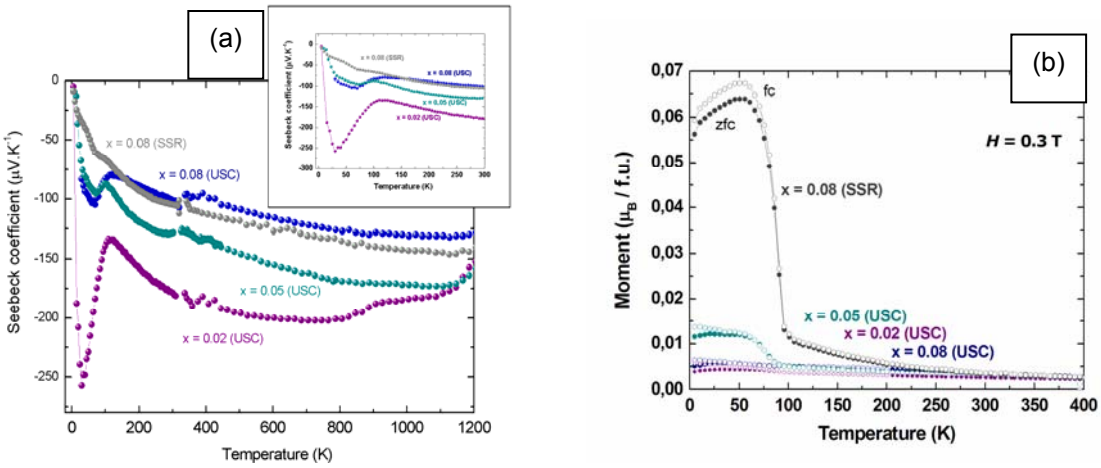

Figure 9 (a) S(T) for $CaMn_{1-x}Nb_xO_3$ (for x = 0.02, 0.05 and 0.08) synthesised by USC (Ultrasonic Spray Combustion) and SSR methods. The inset figure presents S(T) in the low T range (2 K < T < 300 K). Figure 9 (b): The zero field cooled (zfc) and field cooled (fc) magnetizations temperature dependence in a field of H = 0.3 T.

To summarize, an equal Nb substitution leads to a same entropy of charge carriers and therefore same thermopower values for compounds synthesised by both methods (SSR or SC). However SC samples reveal lower resistivity values due to different microstructure than SSR compounds. Combining these two results the power factor presents higher values at equal Nb content for the SC polycrystalline sample. The largest power factor is achieved for the $CaMn_{0.98}Nb_{0.02}O_3$ synthesised by SC synthesis route exhibits $PF_{550K} = 1.77*10^{-4}$ $W.m^{-2}.K^{-1}$ to $PF_{1150K} = 2.05*10^{-4}$ $W.m^{-2}.K^{-1}$.

Thermal conductivity

The thermal conductivity is strongly influenced by the morphology, density, defects and texture of the studied compounds. An important feature consists to determine for the predominant effect considering a specific composition. Thus thermal conductivity studies on single crystal and polycrystalline materials were performed as well as different synthesis methods were used to play with the morphology and microstructure impact.

Higher phonons scattering occurs in a polycrystalline material due to the grain boundaries and the presence of crystalline grains with different orientations. The crystal lattice of a single crystal favours the phonons path through the material and thus contributes to a higher thermal conductivity compared polycrystalline sample (Figure 10). The thermal conductivity ratio between single crystal and polycrystalline material increases from a factor of 2.8 at 300 K to 3.5 at 1000 K. Single crystal presents highest κ values than polycrystalline compounds, and therefore the temperature rise induces a stronger influence on the single crystal / polycrystalline κ values.

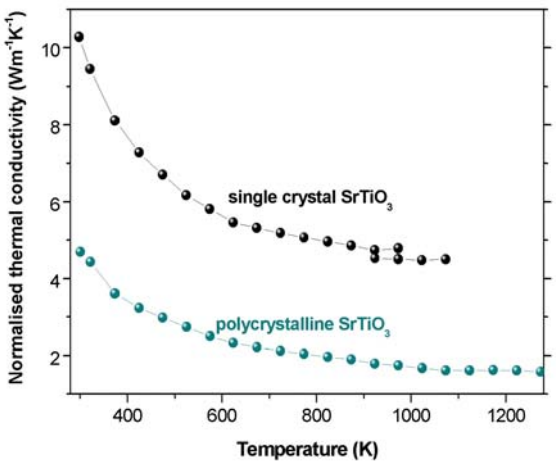

Figure 10: Thermal conductivity temperature dependence of $SrTiO_3$ (insulating compound) for single crystal and polycrystalline SSR sample.

Figure 11 presents the thermal conductivity behaviour at high temperature (300 K < T < 1280 K) for the whole electron-doped manganates series. Predominant carriers are phonons since the electronic component is estimated by negligible from resistivity data using the Wiedemann-Franz law (κ_{el} = Lo Tσ; with Lo the Lorenz number). SSR compounds exhibit thermal conductivity values between 2 to 3 $W.m^{-1}.K^{-1}$ which are typical values for oxide materials. The SSR compounds show a common trend for 300 K < T < 1100 K where κ decreases smoothly with increasing temperature. In this temperature region the electron-doped manganates exhibit semi-metallic like behaviour which can be related to an increase of the electron-phonon and electron-electron scattering leading to a slight heat transport reduction. The SC sample with 2% Nb substitution presents κ < 0.8 -1 $W.m^{-1}.K^{-1}$ up to 1100K. The niobium substitution can be considered as a source of phonons scattering in the Mn sublattice. However different thermal conduction values are reported for compounds synthesized either by SSR or SC methods having the same Nb substitution. Different features as texture, microstructure and porosity could scattered the thermal carriers conduction. The thermal conductivity reduction achieved for SC sample can be explained by phonon scattering effect related to the different microstructures obtained by the SSR and SC methods.

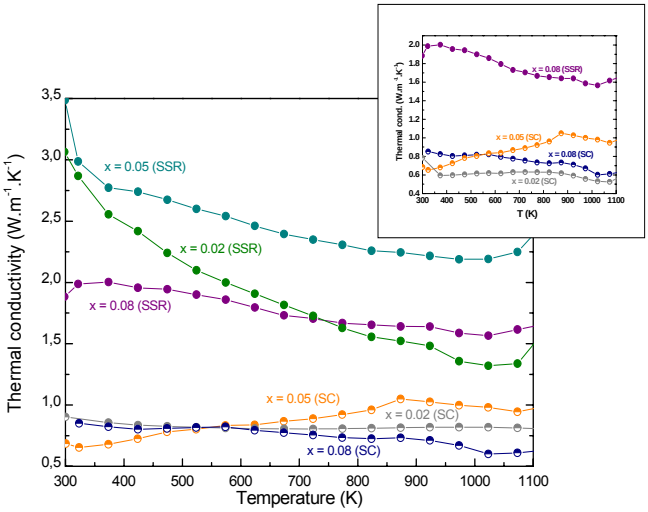

Figure 11: Thermal conductivity temperature dependence for $CaMn_{1-x}Nb_xO_3$ (for x = 0.02, 0.05 and 0.08) synthesised by SSR and SC methods.

Figure of Merit

Figure 12 presents the dimensionless Figure of Merit, *ZT*, of the studied compounds in the high temperature range. The SSR compounds present a maximum ZT value equal to 0.14 at 1040 K for x = 0.02. The best Figure of Merit is reported for the $CaMn_{0.98}Nb_{0.02}O_3$ composition synthesised by SC methods corresponding to a *ZT* = 0.3 at 1040K. A large power factor achieved by slight Nb substitution combined with a microstructure-tuning to lower thermal conduction results in **an improvement of ZT by a factor 2 compared to the SSR compounds**. This Figure of Merit of $ZT_{1040\ K}$= 0.3 corresponds to one of the best ZT value among *n*-type oxide materials where the highest reported ZT is In_2O_3-ZnO doped Y where $ZT_{1073\ K}$ = 0,33 [Isobe 2002]. The electron-doped manganate presents real potential applications for thermoelectric technologies.

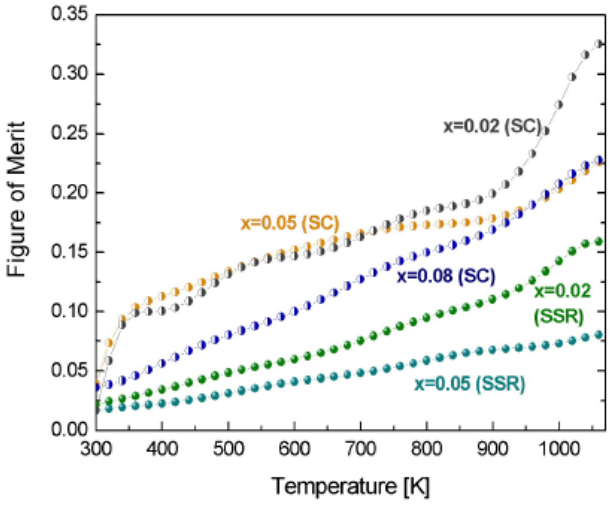

Figure 12: The dimensionless Figure of Merit, *ZT*, temperature dependence for $CaMn_{1-x}Nb_xO_3$ (for x = 0.02, 0.05 and 0.08) synthesised by SSR and SC methods.

Nationale Zusammenarbeit

- Prof. K. Fröhlich, High Voltage Technology Laboratory, ETHZ. Theoretical descriptions correlated with experiments and modelling with A. Bitschi.
- Dr. T. Quan, Laboratory for Nanometallurgy, ETHZ. Thermal conductivity properties on Ni superalloys (Ni-Cr-Co base)-zirconia composites.
- Dr. U. Gonzenbach and Prof. L. Gaukler, Nonmetallic Inorganic Materials, ETHZ. Preparation of particle-stabilized wet foams to form porous thermoelectric *n*-type materials and thermal conductivity measurement of Al_2O_3 porous materials [ref].
- Dr. L. Castaldi and Prof. Ch. Baerlocher, Laboratory of Crystallography ETHZ. High temperature X-ray powder diffraction measurements on manganate-type perovskite structure (up to 1200°C)

Internationale Zusammenarbeit

- Dr. A. Maignan, Dr. S. Hébert, CRISMAT laboratory, UMR 6508 CNRS/ENSICAEN - France. Thermoelectric properties on complex oxide structures at high and low temperatures. *Experimental campaign for low temperature measurements - 2 months (February and March) - Collaboration with CRISMAT (Caen, F.) Thermopower, magnetism and thermal conductivity at low temperature*
- Dr. J. Hejtmanek, Institute of Physics ASCR, Prague - Czech Republic. Thermal properties on oxide materials.

Bewertung 2007 und Ausblick 2008

The electron doped manganate-type phases exhibit large absolute Seebeck coefficients at high temperatures with low resistivity values. Large power factor are achieved combined with low thermal conductivity values make them potential candidates as *n*-type thermoelectric elements. The best TE material (x = 0.02 produced by soft chemistry method) is used as *n*-type legs for the development a Thermoelectric Oxide Module (TOM) and therefore to evaluate the direct manufacturing power of the selected compound. The good results on the thermoelectric manganate-type phases has lead to successful oral or poster presentations on national and international level as well as scientific publications during 2007 (see the list of contributions).

Further measurements on the high temperature (T > 1100 K) behavior of the manganate-type phases will be completed in relation to the phase structural transition. The TEM results on the microstructure of the manganate-type phases reveal interesting features which will be deeply studied to correlate their influence to the transport properties. Additional studies on possible presence of Nb segregation in the USC and SC phases by Electron Energy Loss Spectrometry (EELS) technique are planned to confirm on the atomic level the homogeneity of the compounds.

The research group of Solid State Chemistry and Catalysis acquire the last month a new equipment (Thermal Transport Option for PPMS device) for the measurement of the thermoelectric properties at low temperatures (2 K < T < 400 K).These measurements will allow us to characterize the thermoelectric oxide materials at low temperatures to get a better insight of the thermoelectric properties in the whole temperature range.

Referenzen

[1] [Stambouli 2002] Stambouli A.B.; Traversa E. Renewable and Sustainable Energy Reviews, 6, N° 5 (2002) 433-455

[2] [Nolas] Nolas G. S., Yang J., Goldsmid H. J., Thermal Conductivity - Theory, Properties and Applications, Chapter 1.5, Kluwer Academic / Plenum Publishers, New York, 2004, p. 123.

[3] [Maignan 1998] Maignan A., Martin C., Damay F., Raveau B., Phys. Rev. B 58 (1998) 2758.

[4] [Weidenkaff 2004] Weidenkaff A., Adv. Eng. Mater., 9 (2004) 709.

[5] [Bocher_2007_A] Bocher L., Aguirre M. H., Robert R., Trottmann M., Logvinovich D., Hug P., Weidenkaff A., Thermochim. Acta, 457 (2007) 11.

[6] [Bocher 2007_B] L. Bocher, R. Robert, M. H. Aguirre, S. Malo, S. Hébert, A. Maignan and A. Weidenkaff. Accepted to Solid State Sciences.

[7] [Rietveld 1967] Rietveld H. M., Acta Cryst. 22 (1967) 151.

[8] [Aguirre 2007] Aguirre M. H., Robert R., Logvinovich D., Weidenkaff A., Inorg. Chem., 46 (2007) 2744.

[9] [Hejtmanek 1999] Hejtm\'{a}nek J., Jir\'{a}k Z., Marysko M., Martin C., Maignan A., Hervieu M., Raveau B., Phys. Rev. B 60 (1999) 14057.

List of conference contributions and scientific publications in the 2007 funding period:

- European Solid State Chemistry conference – "*Chimie douce* synthesis methods applied for the development of thermoelectric perovskite-type phases" (poster presentation) -11-13th September 2007
- Swiss Workshop on Materials with Novel Electronic Properties – Manep "Transport properties of electron doped manganates for high temperature thermoelectric applications" (poster presentation) – 28 -30th September 2007.
- PhD day in CRISMAT laboratory as invited speaker on "Synthesis and Characterization of Perovskite-type Oxides for Thermoelectric Technologies" (oral) -6th March 2007.
- TEP-CH symposium on "Synthesis and Thermoelectric Properties of Perovskite-type Manganate Phases" (oral) -15th Mai 2007.
- 5th Empa-PSI PhD student day on "Potential *n*-type oxide materials for thermoelectric technology developments" (oral) – 13th June 2007.

L. Bocher, R. Robert, M. H. Aguirre, S. Malo, S. Hébert, A. Maignan and A. Weidenkaff. Accepted for publication, Solid State Sciences.

M.H. Aguirre, S. Canulescu, R. Robert, N. Homazava, D. Logvinovich, L. Bocher, T. Lippert, M. Doebeli and A. Weidenkaff. Accepted in Journal of Applied Physics (9.11.2007. JAP: MS #JR07-4784)

L. Bocher, M. H. Aguirre, R. Robert, M. Trottmann, D. Logvinovich, P. Hug and A. Weidenkaff. *Thermochimica Acta*, Volume 457, Issues 1-2, 15 June 2007, Pages 11-19

Weidenkaff, A., Robert, R, Aguirre, M.H., Bocher, L., Lippert, T., S. Canulescu, *Renewable Energy*, in press. doi:10.1016/j.renene.2007.05.032

R. Robert, L. Bocher, B. Sipos, M. Döbeli and A. Weidenkaff. *Progress in Solid State Chemistry*, Volume 35, Issues 2-4, 2007, Pages 447-455

A. Weidenkaff, R. Robert, M. H. Aguirre, L. Bocher and L. Schlapbach. *Phys. Stat. Sol.* N°6 (2007) 247-249

R. Robert, M. H. Aguirre, L. Bocher, M. Trottmann, S. Heiroth, Th. Lippert, M. Döbeli, A. Weidenkaff. submitted to Solid State Sciences.